Cell PRESS
Structure
Article

Independent Domain Assembly in a Trapped Folding Intermediate of Multimeric Outer Membrane Secretins

Ingrid Guilvout,[1,2] Mohamed Chami,[3] Elena Disconzi,[1,2,4,5] Nicolas Bayan,[4,5] Anthony P. Pugsley,[1,2,6,*] and Gerard H.M. Huysmans[1,2,6,*]
[1]Molecular Genetics Unit, Departments of Microbiology and of Structural Biology and Chemistry, Institut Pasteur, rue du Dr. Roux, 75724 Paris Cedex 15, France
[2]CNRS ERL3526, rue du Dr. Roux, 75724 Paris Cedex 15, France
[3]C-CINA Center for Cellular Imaging and NanoAnalytics, Biozentrum, University of Basel, 4058 Basel, Switzerland
[4]Institut de Biochimie et de Biophysique Moléculaire et Cellulaire, Université de Paris-Sud, 91405 Orsay, France
[5]CNRS UMR 8619, 91405 Orsay, France
[6]Co-senior author
*Correspondence: max@pasteur.fr (A.P.P.), ghuysman@pasteur.fr (G.H.M.H.)
http://dx.doi.org/10.1016/j.str.2014.02.009

SUMMARY

The outer membrane portal of the *Klebsiella oxytoca* type II secretion system, PulD, is a prototype of a family of proteins, the secretins, which are essential components of many bacterial secretion and pilus assembly machines. PulD is a homododecamer with a periplasmic vestibule and an outer chamber on either side of a membrane-spanning region that is poorly resolved by electron microscopy. Membrane insertion involves the formation of a dodecameric membrane-embedded intermediate. Here, we describe an amino acid substitution in PulD that blocks its assembly at this intermediate "prepore" stage. Electron microscopy indicated that the prepore has an apparently normal periplasmic vestibule but a poorly organized outer chamber. A peptide loop around this amino acid appears to be important for the formation/stability of the fully folded complex. A similar assembly intermediate results from creation of the same amino acid substitution in the *Pseudomonas aeruginosa* secretin XcpQ.

INTRODUCTION

Our understanding of protein folding has benefited greatly from studies of small soluble proteins that often fold in a two-state transition where only the native and unfolded states are populated (Jackson, 1998). It is generally accepted, however, that the majority of proteins (and in particular larger proteins) can also populate alternative conformations and partially structured intermediates (Brockwell and Radford, 2007). The characterization of on-pathway intermediates can reveal structural changes underlying protein folding and assembly.

Novel nuclear magnetic resonance methods have been used to describe the atomic-level structural characteristics of intermediate states at low population levels (Korzhnev et al., 2010; Maity et al., 2005) and can be used to study intermediates that accumulate following changes in solvent or amino acid sequence (Meinhold and Wright, 2011; Neudecker et al., 2012; Religa et al., 2005). In most cases, however, low-resolution spectroscopy is used to provide information on local structural changes occurring during the transient appearance of intermediate states. The intermediate structure is then reconstructed using restraints from experimental validation of sequence variants and/or computational models (Gianni et al., 2010; Gsponer et al., 2006; Vallée-Bélisle and Michnick, 2012).

Folding studies on membrane proteins in phospholipid bilayers have indicated that β-barrel membrane proteins fold via at least one membrane-bound step before attaining their native topology (Huysmans et al., 2010; Kleinschmidt and Tamm, 1996; Rodionova et al., 1995). In addition, many nonconstitutive pore-forming membrane proteins assemble via a well-structured membrane-associated state before they insert fully into the bilayer (Iacovache et al., 2008). Although intermediate states can be isolated efficiently in some cases, their intrinsic metastable nature can make it difficult to solubilize and analyze them in detergents.

PulD forms the outer membrane portal of the *Klebsiella oxytoca* type II pullulanase (PulA) secretion system (T2SS) (Korotkov et al., 2012). It is a multidomain protein (Figure 1) that assembles spontaneously into membranes in vivo and in vitro (self-assembly) (Guilvout et al., 2006, 2008). In vivo- and in vitro-assembled PulD complexes are indistinguishable from each other by all measurable criteria. The ability to self-assemble is shared with all other tested T2SS secretins and with pIV, the secretin encoded by the filamentous *Escherichia coli* bacteriophage f1. However, other classes of secretins from the type III secretion system and the type IV pilus assembly system do not self-assemble under the same conditions (Nickerson et al., 2012).

Previous studies indicated that most of the periplasmic domain (subdomains N_0 to N_2; Figure 1) of PulD is not required for folding to the native state in vivo or in vitro. Indeed, a "minimal PulD" fragment, $PulD^{28–42/259–660}$, consisting primarily of the N_3,

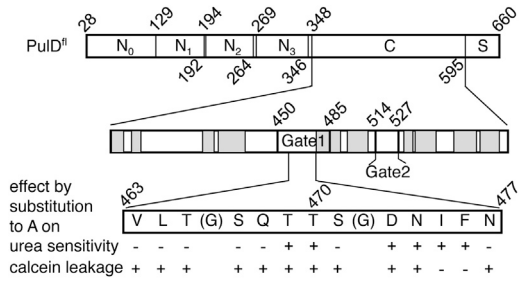

Figure 1. Linear Representation of the PulD Primary Structure

PulD^{fl} represents the domain organization of full-length PulD. Gates 1 and 2 identified in the pIV secretin (Spagnuolo et al., 2010) are indicated following sequence alignment, and transmembrane domains (gray) are shown as predicted by TMBETA (Gromiha and Suwa, 2005). Urea sensitivity and calcein leakage upon replacement of the amino acids shown by alanine are indicated. Numbers shown indicate positions in the amino acid sequence of the features of interest.

C, and S domains (Figure 1), assembles via at least two sequential steps in which rapid dodecamerization is followed by a conformational change concomitant with formation of the native conformation in the membrane (Huysmans et al., 2013). Electron microscopy (EM) of full-length and minimal PulD indicated that the dodecamers consist of two stacked rings (Chami et al., 2005; Nouwen et al., 2000), corresponding respectively to a vestibule that protrudes deep into the periplasm and to an outer chamber.

We previously described the existence of an in vitro assembly intermediate trapped in *di*$C_{16:0}$PC liposomes. However, detailed studies of this intermediate were precluded because it was difficult to extract sufficient quantities from the membranes (Huysmans et al., 2013). Here, we report a PulD variant with characteristics similar to those of the intermediate that can be trapped in *di*$C_{16:0}$PC liposomes (Huysmans et al., 2013). This variant, in which a threonine residue at position 470 was replaced by an isoleucine, was analyzed by EM, spectroscopy, and size fractionation and for its ability to form a secretion channel and a constitutive open pore. The effects of other substitutions at or around T470 were also analyzed, as were the effects of the corresponding substitutions in another secretin of the same family, XcpQ from the T2SS of *Pseudomonas aeruginosa*. The results lead us to propose a role for the peptide located around this threonine residue that forms an essential interaction network to safeguard and coordinate membrane insertion and to protect against premature formation of the pore.

RESULTS

Substitution of T470 in PulD Decreases Multimer Stability In Vivo and In Vitro

Mislocalization of full-length PulD (PulD^{fl}) or PulD$^{28–42/259–660}$ dodecamers to the inner membrane caused by the absence of its dedicated chaperone, PulS (Guilvout et al., 2006), or its signal peptide (Guilvout et al., 2008) is toxic (in the latter case, lethal) for *Escherichia coli* cells. Random mutagenesis of DNA encoding PulD$^{28–42/259–660}$ without its signal peptide led to the isolation and characterization of nontoxic PulD$^{28–42/259–660}$ variants,

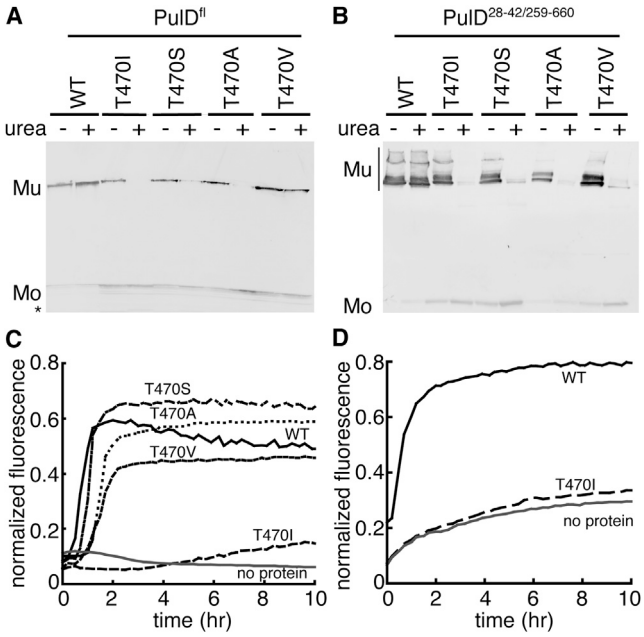

Figure 2. Characterization of PulD^{fl} and PulD$^{28-42/259-660}$T470 Variants

(A and B) SDS-PAGE and immunoblot analysis of the SDS and urea resistance of PulD^{fl} (A) and PulD$^{28–42/259–660}$ (B) multimers produced in vivo and in the presence of lecithin liposomes in vitro, respectively. Mu and Mo indicate multimer and monomer, respectively. *Indicates PulD degradation products. Smears of PulD$^{28–42/259–660}$ multimers likely arise from poor solubilization of membrane clusters.

(C and D) Calcein (C) and carboxyfluorescein (D) leakage of preloaded liposomes upon wild-type (WT) or variant (as indicated) PulD$^{28–42/259–660}$ multimer formation. DNA was omitted from the negative control reaction (no protein).

most of which exhibit drastically reduced ability to form stable multimers (Guilvout et al., 2011). Here, screening of further PulD$^{28–42/259–660}$ variants lacking the signal peptide led us to identify one carrying a T470I substitution in the membrane-embedded C domain (Figure 1) that apparently formed multimers while still allowing cell growth.

The T470I substitution was introduced into PulD^{fl} with its signal peptide. The resulting variant formed multimers, albeit with an apparent lower efficiency than PulD^{fl}WT (Figure 2A). In the presence of PulS, PulD^{fl}T470I associated with the *E. coli* outer membrane (data not shown) but was nonfunctional (unable to restore PulA secretion in a *ΔpulD* mutant; see Experimental Procedures). Because PulD^{fl}T470I was encoded in this assay by a plasmid present at a considerably higher copy number than the chromosomal wild-type (WT) *pulD* allele that it replaced, the result strongly suggests the complete nonfunctionality of PulD^{fl}T470I.

Native PulD dodecamers do not dissociate in SDS or at high urea concentrations (Guilvout et al., 2008; Hardie et al., 1996). However, 4 M urea disrupted the PulD^{fl}T470I dodecamers (Figure 2A). PulD^{fl} in which T470 was replaced by the amino acids S or V, which are physicochemically more similar to T than is I, also formed (partially) urea-sensitive multimers (Figure 2A). However, in contrast to PulD^{fl}T470I, PulD^{fl}T470S and

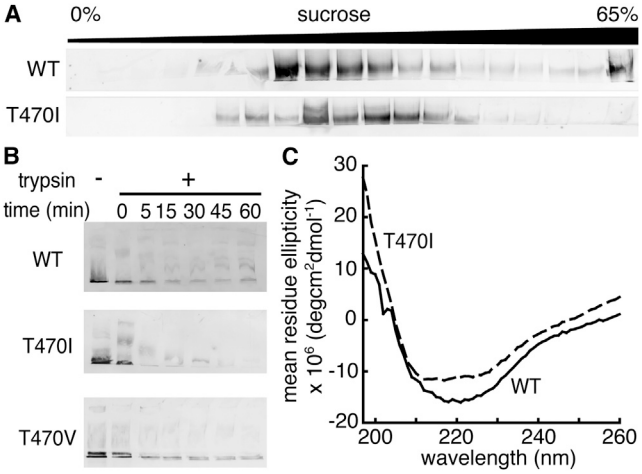

Figure 3. Characterization of In Vitro-Synthesized PulD$^{28–42/259–660}$ WT, T470I, and V Multimers in Lecithin Liposomes

(A) Flotation of WT and PulD$^{28–42/259–660}$T470I multimers through a centrifuged sucrose gradient.

(B) Trypsin sensitivity of PulD$^{28–42/259–660}$WT, T470I, and T470V.

(C) CD spectra of PulD$^{28–42/259–660}$WT and T470I.

Only bands corresponding to multimers are shown in (A) and (B). Monomers comigrate with multimers in (A) and are completely digested in (B).

PulD^{fl}T470V were at least partially functional (30%–70% and 80%–100% PulA secretion, respectively; PulD^{fl}WT secretes 80%–100% PulA).

T470I, S, and V substitutions were introduced into PulD$^{28–42/259–660}$ for in-depth analysis in in vitro translation-assembly reactions (Guilvout et al., 2008, 2011; Huysmans et al., 2013; Nickerson et al., 2012). All three variants formed urea-sensitive multimers when synthesized in vitro in the presence of lecithin liposomes (Figure 2B). PulD$^{28–42/259–660}$T470I multimers were dissociated by urea, as in vivo. Urea also largely dissociated PulD$^{28–42/259–660}$T470S and PulD$^{28–42/259–660}$T470V (Figure 2B).

The ability of the PulD$^{28–42/259–660}$ variants to form a pore was measured by the leakage of self-quenched calcein from preloaded liposomes upon PulD insertion (Disconzi et al., 2014). The fluorescence increase observed following the synthesis of PulD$^{28–42/259–660}$WT, T470V, and T470S indicated efficient calcein leakage from these liposomes due to the formation of a pore (Disconzi et al., 2014), consistent with their ability to promote PulA secretion. Calcein fluorescence remained low upon synthesis of PulD$^{28–42/259–660}$T470I (Figure 2C), indicating the absence of a pore. PulD$^{28–42/259–660}$ T470I also failed to release liposome-encapsulated carboxyfluorescein, a molecule approximately half the size of calcein (Figure 2D).

These data indicate that substitutions of T470 strongly destabilize the PulD dodecamer. Measured by urea sensitivity, the relative stability of the variants followed the same order (WT > T470V ≥ T470S > T470I), irrespective of whether the protein was made in vivo or in vitro. Furthermore, the inability of PulD$^{28–42/259–660}$T470I to promote PulA secretion and to form a pore suggests that the assembly of this variant is incomplete.

PulD$^{28–42/259–660}$T470I Has Features of a Multimeric Folding Intermediate

To determine whether PulD$^{28–42/259–660}$T470I interacts with the lecithin liposomes in the in vitro synthesis reaction, membrane-bound protein was separated from soluble protein and aggregates by flotation through a centrifuged sucrose gradient. The majority of both PulD$^{28–42/259–660}$WT and T470I floated together with the lecithin liposomes to sucrose densities midway through the gradient, with only a small amount remaining at high sucrose densities (Figure 3A). Thus, despite the absence of any measurable pore activity, PulD$^{28–42/259–660}$T470I associated with the liposomes.

We recently described a PulD$^{28–42/259–660}$ assembly intermediate, formed in the presence of *di*C$_{16:0}$PC-liposomes, that is both SDS and trypsin sensitive and that might represent a membrane-embedded prepore with a higher α-helical content than the native dodecamer (urea sensitivity was not determined independently of SDS resistance) (Huysmans et al., 2013). Like this putative prepore, PulD$^{28–42/259–660}$T470I multimers were completely digested by trypsin (Figure 3B). In the case of PulD$^{28–42/259–660}$WT and T470V, however, a trypsin-resistant population persisted even after prolonged incubation, in agreement with their (partial) dissociation by urea and pore activity (Figure 3B). Circular dichroism (CD) spectroscopy showed that PulD$^{28–42/259–660}$T470I has helix-rich features, similar to those of the prepore formed in *di*C$_{16:0}$PC liposomes (Huysmans et al., 2013): a shift of the spectral minimum from 220 nm in the WT protein to 210 nm in the T470I variant (Figure 3C). Consistent with results obtained for PulD$^{28–42/259–660}$WT native and prepore structures (Huysmans et al., 2013), multimers and monomers of PulD$^{28–42/259–660}$T470I could be labeled with transmembrane-specific 1-azidopyrene, indicating that both forms were in contact with the membrane (Figure S1A available online). Thus, trypsin digestion, CD spectroscopy, and transmembrane labeling suggest that lecithin-associated PulD$^{28–42/259–660}$T470I and the putative PulD$^{28–42/259–660}$WT prepore in *di*C$_{16:0}$PC liposomes are in a similar state.

Misfolded or nonassembled monomers could contribute to the observed increased helicity in PulD$^{28–42/259–660}$T470I. To investigate this possibility, PulD$^{28–42/259–660}$ multimers were solubilized in the mild detergent *N*-dodecyl-β-D-maltoside (DDM) and subjected to gel permeation. DDM did not affect the characteristic differences in urea sensitivity and spectral shifts in CD between PulD$^{28–42/259–660}$WT and T470I multimers (Figures S1B and S1C). Monomers coeluted with multimers during gel permeation of PulD$^{28–42/259–660}$T470I in DDM (Figures S1D and S1E). Thus, these monomers probably result from partial dissociation of PulD$^{28–42/259–660}$T470I multimers by SDS after purification, similar to the complete SDS sensitivity of the prepore that forms in vitro in *di*C$_{16:0}$PC liposomes (Huysmans et al., 2013). Therefore, the spectral differences measured between PulD$^{28–42/259–660}$WT and PulD$^{28–42/259–660}$T470I are unlikely to result from the presence of misfolded or nonassembled monomers in the latter.

In conclusion, like the PulD$^{28–42/259–660}$ prepore formed in *di*C$_{16:0}$PC liposomes, PulD$^{28–42/259–660}$T470I forms membrane-associated, (partially) SDS-sensitive and trypsin-sensitive multimers. In contrast, analysis of SDS and trypsin sensitivity suggests that PulD$^{28–42/259–660}$T470V exists as a mixture of native and prepore multimers.

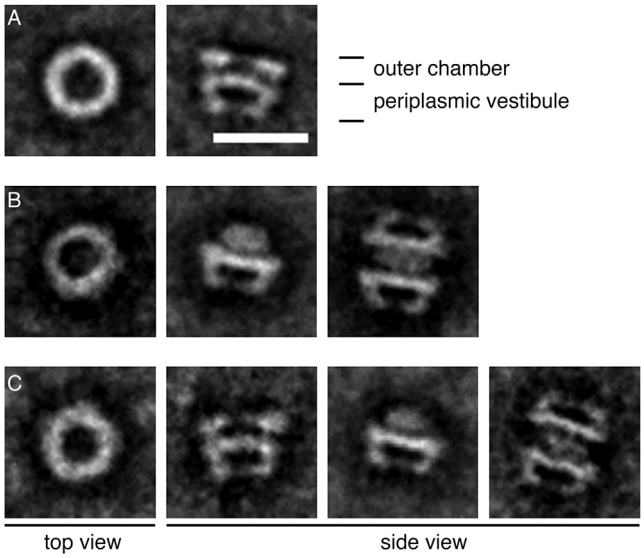

Figure 4. Transmission Electron Microscopy of Negatively Stained PulD$^{28–42/259–660}$WT, T470I, and T470V Solubilized in Dodecylmaltoside

(A) Averaged images of two major classes of PulD$^{28–42/259–660}$WT multimers: top view (left, n = 31) and side view (right, n = 27).

(B) Averaged images of three major classes PulD$^{28–42/259–660}$T470I multimers: top view (left, n = 25) and side view (middle, n = 26) and side view of double complexes (n = 16).

(C) Averaged images of four major classes (left to right) of PulD$^{28–42/259–660}$T470V multimers: top view (left; n = 15), two side views (middle n = 17 and 15 respectively), and double complexes (right; n = 8).

n indicates the number of averaged particles. Scale bar, 15 nm. Field images and a gallery of all classes are shown in Figure S2.

Negative-Stain EM of PulD$^{28–42/259–660}$T470 Variants

EM was used to analyze structural differences between PulD$^{28–42/259–660}$WT and PulD$^{28–42/259–660}$T470I solubilized in DDM. Previous EM analyses of PulD dodecamers in the detergent Zwittergent 3-14 revealed particles composed of two stacked rings corresponding to the periplasmic N-domain vestibule and the outer chamber (Chami et al., 2005; Nouwen et al., 2000). Projections of PulD$^{28–42/259–660}$WT multimers in DDM (Figure 4A) were indistinguishable from those obtained in Zwittergent 3-14. Although particles of PulD$^{28–42/259–660}$T470I appeared as typical circular structures when viewed parallel to the symmetry axis ("top view"), analysis of perpendicular projections ("side view") revealed two classes of particles, one corresponding to single PulD$^{28–42/259–660}$T470I multimers and one to symmetrical dimers of multimers that were clearly different from PulD$^{28–42/259–660}$WT (Figure 4B). In both classes, the density corresponding to the periplasmic vestibule remained unaltered, whereas that corresponding the outer chamber appeared poorly organized or collapsed. The space between the periplasmic vestibules in particles containing a dimer of multimers likely contained the poorly organized part of the C domains that form the outer chamber (Figure 4B). Consistent with the (at least) partial SDS, urea, and trypsin resistance of PulD$^{28–42/259–660}$T470V, analysis of side views visualized by EM indicated a mixture of some particles resembling those formed by PulD$^{28–42/259–660}$T470I and by PulD$^{28–42/259–660}$WT (Figure 4C).

PulD$^{28–42/259–660}$ Stability Is Sensitive to Substitutions around T470

The T470 substitution is the only one identified so far with a measurable effect on multimer stability by the methodology applied here (Guilvout et al., 2011). Alignment of the PulD amino acid sequence with those of known self-assembly secretins (Nickerson et al., 2012) indicated that T470 lies in the middle of a poorly conserved sequence from V463 to N477 (Figure S3), in a region predicted to lack regular secondary structure and that, in the secretin pIV, is thought to play a role in channel gating (gate 1) (Spagnuolo et al., 2010) (Figure 1). We investigated whether other residues in this peptide also influenced the stability of the PulD$^{28–42/259–660}$ native state by individually substituting all of them (except G) by A (Figure 1). Multimers carrying a T470-by-A substitution were urea sensitive (both in vivo and in vitro; Figures 2A and 2B), partially functional in the PulA secretion assay (30%–70% of WT secretion), and permeabilized calcein-containing liposomes in vitro (Figure 2C). Substitution of residues preceding T469 resulted in multimers indistinguishable from those formed by PulD$^{28-42/259-660}$WT (urea resistant and promoting calcein leakage; Figure 1). In contrast, with the exception of S471, substitution of residues T469 through F476 resulted in urea-sensitive multimers (Figure 1). Like PulD$^{28–42/259–660}$T470A, all of these variants facilitated calcein efflux, with the exception of PulD$^{28–42/259–660}$I475A and F476A (Figure 1), both of which also failed to promote carboxyfluorescein leakage (not shown). Because structure predictions suggest that I475 and F476 are close to a potential β strand (TMBETA-NET; Gromiha and Suwa, 2005; Figure 1), we could not exclude that these substitutions substantially perturb PulD folding. Overall, the data indicate that substitutions between T469 and F476 cause profound effects on PulD multimer stability.

To examine this phenomenon further, G472 was replaced by the larger aliphatic amino acids A and I and by P. PulD$^{28–42/259–660}$G472A was urea resistant and allowed calcein efflux (Figures 5A and 5B). PulD$^{28–42/259–660}$G472I and G472P formed urea-sensitive multimers that did not promote efficient calcein or carboxyfluorescein efflux (Figures 5A–5C). To investigate whether chain flexibility introduced by G472 is an important factor in attaining the PulD native state, four neighboring residues (T470, S471, D473, and N474) were replaced by G. PulD$^{28–42/259–660}$G$_{470–474}$ was partially urea sensitive (Figure 5A) but allowed calcein efflux from liposomes (Figure 5D), suggesting that chain flexibility indeed contributes to formation of the PulD native state, but also that residue specific interactions establish the unusual high stability that is characteristic of secretin. Together, these results demonstrate the role of a non-conserved, flexible, and apparently nonstructured peptide in attaining and stabilizing the PulD native state.

Equivalent Substitutions in XcpQ Lead to Prepore Formation

We next investigated whether this region is also important for stabilizing the native state of the PulD homolog XcpQ from *P. aeruginosa* by creating the equivalent of the highly destabilizing T470-substitutions in PulD at residue T478 in XcpQ (Figure S3). XcpQ WT formed SDS- and urea-resistant multimers (Figure 6A) and allowed carboxyfluorescein leakage from liposomes through a constitutively open pore (that does not allow

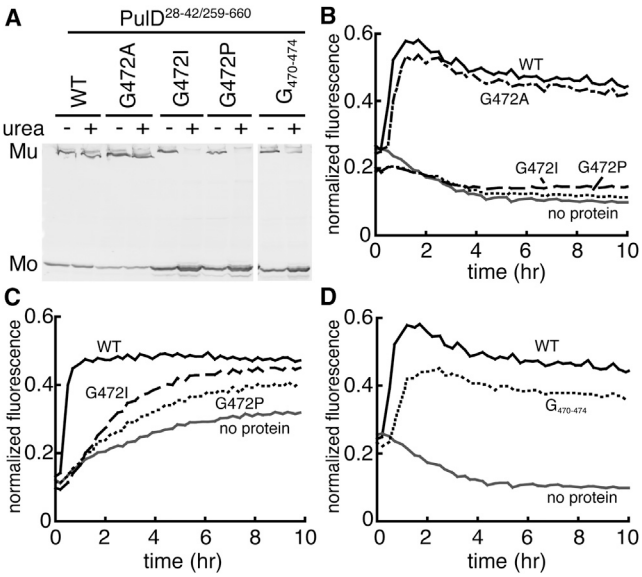

Figure 5. Characterization of In Vitro-Synthesized PulD$^{28–42/259–660}$ Glycine Variants

(A) SDS-PAGE and immunoblot analysis of the SDS and urea resistance of variants PulD$^{28–42/259–660}$ multimers as indicated. Mu and Mo indicate multimer and monomer, respectively.

(B and C) Calcein and carboxyfluorescein leakage, respectively, from preloaded liposomes upon multimerization of single G variants of PulD$^{28–42/259–660}$.

(D) Calcein leakage of preloaded liposomes upon multimerization of PulD$^{28–42/259–660}$G$_{470–474}$. DNA was omitted from the negative control reaction (no protein).

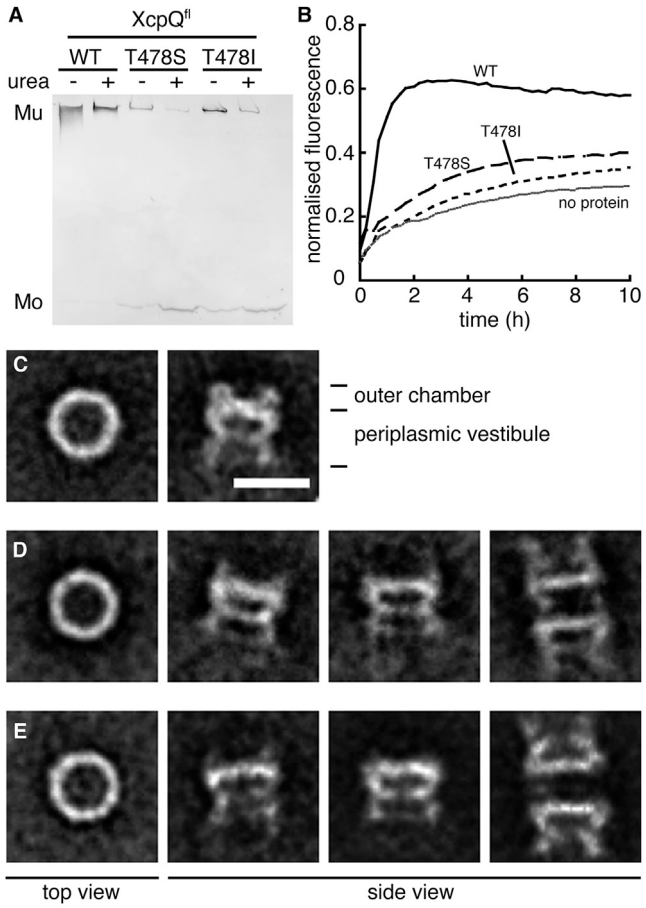

Figure 6. Characterization of In Vitro-Synthesized XcpQ Multimers

(A) SDS-PAGE and immunoblot analysis of the SDS and urea resistance of WT and variant XcpQ multimers as indicated. Mu and Mo indicate multimer and monomer, respectively.

(B) Carboxyfluorescein leakage from preloaded liposomes upon multimerization of WT or variant XcpQ. DNA was omitted from the negative control (no protein).

(C) Averaged images of two major classes of XcpQ WT multimers: top view (left, n = 10) and side view (right, n = 24).

(D) Averaged images of four major classes of XcpQ T478I multimers: top view (left, n = 15), two side views (middle, n = 23 and 13, respectively), and double complexes (n = 21).

(E) Averaged images of four classes of XcpQ T478S multimers: top view (left; n= 9), two side views (middle; n = 11), and double complexes (n = 31).

n indicates the number of averaged particles. Scale bar, 15 nm. A gallery of all classes is shown in Figure S4. In (C)–(E), XcpQ multimers were solubilized in dodecylmaltoside prior to analysis.

calcein efflux) (Figure 6B) (Disconzi et al., 2014; Nickerson et al., 2012). XcpQ T478I formed partially SDS-resistant multimers that were dissociated upon urea treatment (Figure 6A) and did not allow carboxyfluorescein leakage (Figure 6B), suggesting that the normally constitutively open pore was not formed. EM comparisons of XcpQ WT and T478I provided unprecedented views of the XcpQ secretin. In top views, XcpQ WT particles appeared as rings (Figure 6C). In side views, XcpQ WT appeared as two stacked rings (Figure 6C). The larger of these two rings contained a constriction at midlength and corresponds to the periplasmic vestibule. This vestibule includes the N_0, N_1, and N_2 domains that were visible in EM images of ETEC GspD (Reichow et al., 2010), but not in PulD^{fl} (Chami et al., 2005; Nouwen et al., 2000). The thinner ring comprises the outer chamber, as it does in PulD (Figure 6C). It was less well defined in the T478I variant (Figure 6D), although the effect of the substitution was less dramatic than in PulD$^{28–42/259–660}$. Replacement of XcpQ residue T478 by S resulted in multimers that were SDS resistant and partially urea sensitive (as in PulD$^{28–42/259–660}$) but did not leak carboxyfluorescein (Figures 6A and 6B). Both XcpQ variants also sorted into an additional class of particles containing two secretin multimers (Figures 6D and 6E). Overall, the EM analysis revealed that the outer chambers were poorly structured in XcpQ T478I and T478S variants and that the T478S substitution was more detrimental to the XcpQ structure than T478I (Figure 6E). Although the extent of the structural deformations caused of these two substitutions in XcpQ are the reverse of those they caused in PulD$^{28–42/259–660}$, the data reveal an unexpected role for this threonine in both secretins, suggesting that, despite its poor conservation (Figure S3), they play a vital role in one of the final steps toward the secretin native state.

DISCUSSION

PulD is a multidomain protein that assembles in vitro through membrane driven dodecamerization, followed by the formation of a putative prepore structure and a conformational switch to the native state (Huysmans et al., 2013). Here, the structure of the putative prepore was isolated by progressive destabilization

of the native state via substitution of T470 to V, S, and I. EM revealed that these substitutions do not affect the periplasmic vestibule but cause disorder in the C domain that includes the transmembrane segments and forms the outer chamber. Small molecules do not permeate through these prepore structures, confirming that they do not possess the constitutively open pore that is present in the native PulD structure (Disconzi et al., 2014). The fact that homologous substitutions in the secretin XcpQ have similar effects indicates that this mechanism is not specific to PulD.

Visualization of prepore structures by EM provides insight into the mechanism of secretin assembly. In $PulD^{fl}$ and related secretins, the walls of the vestibule are formed by the N domains (N_0 to N_3 in $PulD^{fl}$) (Chami et al., 2005; McLaughlin et al., 2012). $PulD^{28–42/259–660}$ contains only the N_3 domain, which is predicted to form a structure similar to the globular domains N_1 and N_2 (Korotkov et al., 2009; Spreter et al., 2009; Van der Meeren et al., 2013). Docking of the N_3 domain in EM structures of the related secretin from ETEC places the N_3 domain in the wall at the base of the vestibule close to the membrane (Reichow et al., 2010). Two independent observations support the idea that N_3 domains contribute directly to PulD-assembly: (1) the C domain that closes off the vestibule near the membrane cannot multimerize independently of the N_3 domain (Guilvout et al., 1999, 2008) and (2) we show here that the vestibule is assembled in the prepore. Thus, although the disorder in the C domain of a blocked prepore is unlikely to provide sufficient stable interactions to support multimer assembly, we propose that the N domains fold independently of the C domains and facilitate oligomerization into a dodecameric structure by organizing the C domains. As in many pore-forming proteins, a conformational change in the C domain could then be responsible for the final steps in PulD assembly that occur before full membrane insertion (Dunstone and Tweten, 2012; Tilley and Saibil, 2006).

The effects of sequence changes in PulD (Disconzi et al., 2014; Guilvout et al., 1999, 2008, 2011) and related secretins (Chen et al., 2004; Frye et al., 2006; Helm et al., 2007; Spagnuolo et al., 2010) have provided insight into the function, structure, assembly, and stability of these elusive complexes. However, these studies failed to identify polypeptide regions with a measurable contribution to secretin stability and assembly, as determined by methods traditionally used to assess these parameters. Indeed, all PulD sequence variants characterized hitherto either formed stable multimeric complexes indistinguishable from the WT protein or were substantially defective in multimerization (Disconzi et al., 2014; Guilvout et al., 1999, 2008, 2011). The urea-sensitive, partially SDS-resistant PulD variant carrying the T470I substitution has a measurable contribution to secretin stability and assembly. In PulD, T470 lies in the middle of a poorly conserved peptide that is predicted to have limited structure. Therefore, it might be considered surprising that substitution of T470 to I blocks a late stage in secretin assembly. Mild substitutions of the residues flanking T470 identify a continuous subset of amino acids that also modulate PulD stability. Intriguingly, whereas residue-specific interactions appear to be important for high PulD stability, membrane insertion appears to rely only on the flexibility of the peptide. Indeed, despite the fact that replacing the peptide by a glycine linker substantially destabilized PulD, it did not prevent pore formation. These results hint at a more important role for this peptide in facilitating PulD membrane insertion. Peptide flexibility could facilitate interactions between other segments of PulD and assembly arrests if these interactions cannot be created. Such a mechanism would be reminiscent of that proposed as the basis of the misfolding caused by disease-related modifications in the cystic fibrosis transmembrane conductance regulators (Mendoza et al., 2012). Alternatively, substitutions in the peptide around T470 might block a conformational switch that facilitates membrane insertion. Interestingly, the peptide is located within a region (gate 1) that is proposed to play a role in the gating of the pIV secretin (Spagnuolo et al., 2010). Gate regions could have a role in secretin assembly, because PulD does not multimerize when gate 1 is deleted (Disconzi et al., 2014; Spagnuolo et al., 2010). Constitutively open secretin channels would be lethal to the bacterium (due to occasional mislocalization to the inner membrane) unless they are tightly closed. Therefore, assembly of gate 1 could be a prerequisite for membrane insertion. Such a mechanism is remarkably similar to that recently proposed for the assembly of aerolysin, a heptameric bacterial toxin, in which the flexibility of a pre-stem loop drives increased intermonomer contacts and prepore-pore transitions (Degiacomi et al., 2013).

In conclusion, we show how genetic screening in combination with biochemical and biophysical analysis can provide valuable insights into the architecture and assembly of complex membrane proteins for which high-resolution structural details are lacking.

EXPERIMENTAL PROCEDURES

Strains, Plasmids, Site-Directed Mutagenesis, Growth Conditions, and Secretion Assays

E. coli K-12 PAP105 [Δ(*lac-pro*) F′ (*lacI*^{q1} Δ*lacZM15 proAB*$^{+}$ Tn*10*)] was used for cloning, site-directed mutagenesis and in vivo PulD assembly experiments. *E. coli* MC4100 derivative PAP7447 (Hardie et al., 1996; F′ *lacI*^{q1} *pro*$^{+}$ Tn*10*), with *pulS, pulA*, and *pulC-O* integrated into *malPp* and with a large deletion in *pulD*, was used for secretion assays. All strains were grown at 30°C in Luria-Bertani broth supplemented with the appropriate antibiotics (ampicillin at 100 μg/ml and chloramphenicol at 25 μg/ml).

pCHAP3727 containing the *pullD*$^{28–42/259–660}$ gene carrying the spontaneous T470I substitution was extracted from an IPTG induced *E. coli* BL21 strain carrying pCHAP3716 (Guilvout et al., 2008). Site-directed mutagenesis was performed on pCHAP3716 (Guilvout et al., 2008) and pHH43 (Hoang et al., 2011) for the construction of $PulD^{28–42/259–660}$ and XcpQ variants, respectively. Oligonucleotides (Sigma Genosys) used in site-directed mutagenesis are listed in Table S1. Substitutions were introduced into full-length PulD for in vivo studies by exchanging the region carrying the mutation in *pulD*$^{28–42/259–660}$ with the WT region in *pulD*$^{1–660}$ on pSU18 (pCHAP3635; Guilvout et al., 1999) utilizing restriction endonucleases HpaI and BlpI for T470S and T470V and NaeI and BlpI for T470A (resulting in the plasmids pCHAP3995, pCHAP3301, and pCHAP3996, respectively). Substitution T470I was first introduced in pUC18 *pulD*$^{1–660}$ (pCHAP3671; Guilvout et al., 1999) using AgeI and StuI to yield pCHAP3732 and then ligated into pSU18 cut with EcoRI and HindIII (to give pCHAP3910). All constructs were sequenced (Beckman).

Pullulanase secretion assays were performed as described previously (Michaelis et al., 1985). The level of secretion is the percentage of the total amount of pullulanase that is detected in unlysed cells. To analyze PulD assembly in vivo, pSU18 carrying WT or mutant *pulD* was cotransformed with a plasmid carrying the gene for its cognate chaperone PulS (pCHAP585; Guilvout et al., 1999).

In Vitro Transcription, Translation, and Permeability Assays

PulD$^{28–42/259–660}$WT or XcpQ WT and their variants were produced in a coupled transcription-translation reaction (RTS 100 *E. coli* HY kit, 5Prime) supplemented with the appropriate plasmid DNA and artificial liposomes (Guilvout et al., 2008). Synthesis and assembly was allowed to continue for 6 hr at 30°C. Pore formation was monitored by leakage of self-quenched calcein or carboxyfluorescein, previously incorporated into the liposomes, as described elsewhere (Disconzi et al., 2014). Briefly, 1,2-dioleoyl-*sn*-glycero-3-phosphocholine (Avanti Polar Lipids) liposomes were hydrated in 50 mM TrisCl (pH 7.4) containing either 50 mM calcein or 10 mM carboxyfluorescein. Liposomes were sonicated to obtain unilamellar liposomes. Non-incorporated fluorescent molecules were eliminated by dialysis against buffer (3 × 2L). Secretin synthesis and assembly was monitored for 10 hr in an Infinitive F200 Pro Tecan spectrofluorometer at 30°C with continuous shaking. Fluorescence was normalized using the total amount of fluorescence upon the addition of 0.1% Triton X-100.

SDS-PAGE and Western Blotting

Monomeric and multimeric forms of PulD and XcpQ (WT or variants) were separated in SDS on a 4%–10% discontinuous polyacrylamide (37.5:1 acrylamide/bis-acrylamide) gel and analyzed by immunoblotting after transfer to nitrocellulose membranes (GE Healthcare) using an antibody against PulD or XcpQ multimers, as appropriate (or by Coomassie staining of the gel in permeability assays; Disconzi et al., 2014). Prior to migration, samples were mixed 1:1 with SDS-PAGE loading buffer (4% SDS, 125 mM Tris [pH 6.8], 20% glycerol). In vivo multimer formation was analyzed on a 3%/4%/10% discontinuous polyacrylamide gel to separate aggregates from multimeric forms.

Protein Solubilization

Liposomes containing PulD$^{28–42/259–660}$WT, XcpQ WT, or their variants were washed twice with 25 mM Tris (pH 7.2) and collected by centrifugation (15 min, 55,000 × *g*). Purified liposomes were resuspended in 100 mM Tris (pH 7.5) and 500 mM NaCl and diluted twice in 2% DDM. The lipid to detergent ratio was typically 1:5 (w/w) for solubilization.

Urea Treatment

Urea resistance of in vivo produced PulD^{fl}WT and its variants was assayed by resuspension of equal amounts of cells in 25 mM Tris (pH 7.2), with or without 4 M urea, followed by incubation for 1 hr at room temperature. PulD$^{28–42/259–660}$WT, XcpQ WT, and their variants synthesized in vitro were treated accordingly, with the exception that aliquots from the synthesis reaction (or of DDM solubilized samples) were mixed 1:1 with buffer containing 0 or 8 M urea to obtain final urea concentrations of 0 and 4 M in the treated samples, respectively. All samples were analyzed by SDS-PAGE and immunoblotting.

Trypsin Treatment

Liposomes containing PulD$^{28–42/259–660}$WT or its variants were harvested by centrifugation (15 min, 55,000 × *g*) and resuspended in 50 mM Tris (pH 7.5) and 250 mM NaCl (to one-third of the original volume). The protein concentration was equalized in each sample before limited proteolysis using trypsin (25:1 mol PulD/mol trypsin) at room temperature. Aliquots were removed at time intervals after trypsin addition. Proteolysis was terminated with 8 mM Pefabloc (Interchim) before analysis by SDS-PAGE and immunoblotting.

Flotation of Liposomes on a Discontinuous Sucrose Gradient

Liposomes containing PulD$^{28–42/259–660}$WT or its variants were collected by centrifugation (15 min, 55,000 × *g*) and resuspended in 65% w/v sucrose in 25 mM Tris (pH 7.2). Samples (100 μl) were overlaid with 60%, 40%, 20%, and 0% sucrose in the same buffer. Liposomes were floated by centrifugation for 2 hr at 150,000 × *g*. Fractions (150 μl) were taken from the top and analyzed by SDS-PAGE and immunoblotting.

Analytical Gel Permeation

Analytical gel permeation of PulD$^{28–42/259–660}$WT and T470I was performed on protein produced for 24 hr in an RTS 500 *E. coli* HY kit (5Prime) to obtain good yields. Liposomes were washed and PulD$^{28–42/259–660}$ was solubilized in 1% DDM in 50 mM CAPS (pH 10), 250 mM NaCl, because multimers, which ran close to the void volume in Tris buffer (not shown), were included better in the matrix of the Superose 6 column. Fractions were mixed with SDS-loading buffer and analyzed by SDS-PAGE and immunoblotting.

1-Azidopyrene Labeling

PulD$^{28–42/259–660}$WT, T470I, and T470V were labeled as described previously (Huysmans et al., 2013). Briefly, PulD$^{28–42/259–660}$ synthesized in the presence of lecithin and pelleted (13,000 × *g*, 1 hr) was washed twice in 50 mM sodium phosphate buffer (pH 8.0), collected by centrifugation (13,000 × *g*, 1 hr). Sedimented liposomes were resuspended in 100 ml of the same buffer containing 250 mM NaCl and 1 mM 1-azidopyrene (from a 200 mM stock solution in dimethylsulfoxide; Hangzhou Sage Chemical). Samples were shaken for 1 hr, followed by UV irradiation for 15 min (312 nm), centrifugation (13,000 × *g*, 1 hr), resuspension in SDS-loading buffer, and electrophoresis in SDS on a 4%–15% polyacrylamide gel (Bio-Rad). Protein bands were visualized under UV light (312 nm) and by immunoblotting.

CD Spectroscopy

Spectra of PulD$^{28–42/259–660}$WT and T470I in liposomes were obtained after washing the synthesis reactions as above and resuspension of the samples to 0.8 mg protein/ml. Spectra in DDM were taken after protein solubilization as above and removal of nonsolubilized material by centrifugation (100,000 × *g*, 30 min). Typically 10%–15% of the protein was recovered from the liposomes. CD spectra were taken on an AVIV spectrometer between 200 and 260 nm at a rate of 20 nm/min and a bandwidth of 1 nm in a 0.2 mm cuvette. Spectra were averaged over three measurements and the appropriate buffer spectra were subtracted.

Transmission Electron Microscopy and Image Processing

For negative staining, aliquots of 5 μl of sample were adsorbed on the carbon film-coated copper grids, washed with three droplets of pure water, and subsequently stained with 2% uranyl-acetate. Images were recorded on a Veleta 2K × 2K CCD camera (Olympus, Germany) using a Philips CM10 TEM operating at 80 keV. For image processing, reference-free alignment was performed on manually selected particles from digitized electron micrographs using the EMAN image-processing package (Ludtke et al., 1999). Then, particle projections were classified by multivariant statistical analysis. The class averages with the best signal-to-noise ratio were selected and gathered in a gallery.

SUPPLEMENTAL INFORMATION

Supplemental Information includes four figures and one table and can be found with this article online at http://dx.doi.org/10.1016/j.str.2014.02.009.

ACKNOWLEDGMENTS

We thank Patrick England and Bruno Baron for assistance with circular dichroism and Prof. Henning Stahlberg (Biozentrum, University of Basel) for his continued support. This work was funded in part by the French National Research Agency (ANR grant number 09-BLAN-0291). G.H.M.H. was a recipient of a Marie Curie Intra-European Fellowship (PIEF-GA-2010-272611) and an EMBO-Pasteur fellowship (ALTF 1088-2010). The EM work was supported in part by the Swiss National Science Foundation (SystemsX.ch RTD CINA).

Received: November 11, 2013
Revised: January 27, 2014
Accepted: February 11, 2014
Published: March 20, 2014

REFERENCES

Brockwell, D.J., and Radford, S.E. (2007). Intermediates: ubiquitous species on folding energy landscapes? Curr. Opin. Struct. Biol. *17*, 30–37.

Chami, M., Guilvout, I., Gregorini, M., Rémigy, H.W., Müller, S.A., Valerio, M., Engel, A., Pugsley, A.P., and Bayan, N. (2005). Structural insights into the secretin PulD and its trypsin-resistant core. J. Biol. Chem. *280*, 37732–37741.

Chen, C.J., Tobiason, D.M., Thomas, C.E., Shafer, W.M., Seifert, H.S., and Sparling, P.F. (2004). A mutant form of the Neisseria gonorrhoeae pilus secretin protein PilQ allows increased entry of heme and antimicrobial compounds. J. Bacteriol. *186*, 730–739.

Degiacomi, M.T., Iacovache, I., Pernot, L., Chami, M., Kudryashev, M., Stahlberg, H., van der Goot, F.G., and Dal Peraro, M. (2013). Molecular assembly of the aerolysin pore reveals a swirling membrane-insertion mechanism. Nat. Chem. Biol. *9*, 623–629.

Disconzi, E., Guilvout, I., Chami, M., Masi, M., Huysmans, G.H., Pugsley, A.P., and Bayan, N. (2014). Bacterial secretins form constitutively open pores akin to general porins. J. Bacteriol. *196*, 121–128.

Dunstone, M.A., and Tweten, R.K. (2012). Packing a punch: the mechanism of pore formation by cholesterol dependent cytolysins and membrane attack complex/perforin-like proteins. Curr. Opin. Struct. Biol. *22*, 342–349.

Frye, S.A., Assalkhou, R., Collins, R.F., Ford, R.C., Petersson, C., Derrick, J.P., and Tønjum, T. (2006). Topology of the outer-membrane secretin PilQ from Neisseria meningitidis. Microbiology *152*, 3751–3764.

Gianni, S., Ivarsson, Y., De Simone, A., Travaglini-Allocatelli, C., Brunori, M., and Vendruscolo, M. (2010). Structural characterization of a misfolded intermediate populated during the folding process of a PDZ domain. Nat. Struct. Mol. Biol. *17*, 1431–1437.

Gromiha, M.M., and Suwa, M. (2005). A simple statistical method for discriminating outer membrane proteins with better accuracy. Bioinformatics *21*, 961–968.

Gsponer, J., Hopearuoho, H., Whittaker, S.B., Spence, G.R., Moore, G.R., Paci, E., Radford, S.E., and Vendruscolo, M. (2006). Determination of an ensemble of structures representing the intermediate state of the bacterial immunity protein Im7. Proc. Natl. Acad. Sci. USA *103*, 99–104.

Guilvout, I., Hardie, K.R., Sauvonnet, N., and Pugsley, A.P. (1999). Genetic dissection of the outer membrane secretin PulD: are there distinct domains for multimerization and secretion specificity? J. Bacteriol. *181*, 7212–7220.

Guilvout, I., Chami, M., Engel, A., Pugsley, A.P., and Bayan, N. (2006). Bacterial outer membrane secretin PulD assembles and inserts into the inner membrane in the absence of its pilotin. EMBO J. *25*, 5241–5249.

Guilvout, I., Chami, M., Berrier, C., Ghazi, A., Engel, A., Pugsley, A.P., and Bayan, N. (2008). In vitro multimerization and membrane insertion of bacterial outer membrane secretin PulD. J. Mol. Biol. *382*, 13–23.

Guilvout, I., Nickerson, N.N., Chami, M., and Pugsley, A.P. (2011). Multimerization-defective variants of dodecameric secretin PulD. Res. Microbiol. *162*, 180–190.

Hardie, K.R., Lory, S., and Pugsley, A.P. (1996). Insertion of an outer membrane protein in Escherichia coli requires a chaperone-like protein. EMBO J. *15*, 978–988.

Helm, R.A., Barnhart, M.M., and Seifert, H.S. (2007). pilQ Missense mutations have diverse effects on PilQ multimer formation, piliation, and pilus function in Neisseria gonorrhoeae. J. Bacteriol. *189*, 3198–3207.

Hoang, H.H., Nickerson, N.N., Lee, V.T., Kazimirova, A., Chami, M., Pugsley, A.P., and Lory, S. (2011). Outer membrane targeting of Pseudomonas aeruginosa proteins shows variable dependence on the components of Bam and Lol machineries. MBio. *2*, e00246-11.

Huysmans, G.H., Baldwin, S.A., Brockwell, D.J., and Radford, S.E. (2010). The transition state for folding of an outer membrane protein. Proc. Natl. Acad. Sci. USA *107*, 4099–4104.

Huysmans, G.H., Guilvout, I., and Pugsley, A.P. (2013). Sequential steps in the assembly of the multimeric outer membrane secretin PulD. J. Biol. Chem. *288*, 30700–30707.

Iacovache, I., van der Goot, F.G., and Pernot, L. (2008). Pore formation: an ancient yet complex form of attack. Biochim. Biophys. Acta *1778*, 1611–1623.

Jackson, S.E. (1998). How do small single-domain proteins fold? Fold. Des. *3*, R81–R91.

Kleinschmidt, J.H., and Tamm, L.K. (1996). Folding intermediates of a beta-barrel membrane protein. Kinetic evidence for a multi-step membrane insertion mechanism. Biochemistry *35*, 12993–13000.

Korotkov, K.V., Pardon, E., Steyaert, J., and Hol, W.G. (2009). Crystal structure of the N-terminal domain of the secretin GspD from ETEC determined with the assistance of a nanobody. Structure *17*, 255–265.

Korotkov, K.V., Sandkvist, M., and Hol, W.G. (2012). The type II secretion system: biogenesis, molecular architecture and mechanism. Nat. Rev. Microbiol. *10*, 336–351.

Korzhnev, D.M., Religa, T.L., Banachewicz, W., Fersht, A.R., and Kay, L.E. (2010). A transient and low-populated protein-folding intermediate at atomic resolution. Science *329*, 1312–1316.

Ludtke, S.J., Baldwin, P.R., and Chiu, W. (1999). EMAN: semiautomated software for high-resolution single-particle reconstructions. J. Struct. Biol. *128*, 82–97.

Maity, H., Maity, M., Krishna, M.M., Mayne, L., and Englander, S.W. (2005). Protein folding: the stepwise assembly of foldon units. Proc. Natl. Acad. Sci. USA *102*, 4741–4746.

McLaughlin, L.S., Haft, R.J., and Forest, K.T. (2012). Structural insights into the Type II secretion nanomachine. Curr. Opin. Struct. Biol. *22*, 208–216.

Meinhold, D.W., and Wright, P.E. (2011). Measurement of protein unfolding/refolding kinetics and structural characterization of hidden intermediates by NMR relaxation dispersion. Proc. Natl. Acad. Sci. USA *108*, 9078–9083.

Mendoza, J.L., Schmidt, A., Li, Q., Nuvaga, E., Barrett, T., Bridges, R.J., Feranchak, A.P., Brautigam, C.A., and Thomas, P.J. (2012). Requirements for efficient correction of ΔF508 CFTR revealed by analyses of evolved sequences. Cell *148*, 164–174.

Michaelis, S., Chapon, C., D'Enfert, C., Pugsley, A.P., and Schwartz, M. (1985). Characterization and expression of the structural gene for pullulanase, a maltose-inducible secreted protein of Klebsiella pneumoniae. J. Bacteriol. *164*, 633–638.

Neudecker, P., Robustelli, P., Cavalli, A., Walsh, P., Lundström, P., Zarrine-Afsar, A., Sharpe, S., Vendruscolo, M., and Kay, L.E. (2012). Structure of an intermediate state in protein folding and aggregation. Science *336*, 362–366.

Nickerson, N.N., Abby, S.S., Rocha, E.P., Chami, M., and Pugsley, A.P. (2012). A single amino acid substitution changes the self-assembly status of a type IV piliation secretin. J. Bacteriol. *194*, 4951–4958.

Nouwen, N., Stahlberg, H., Pugsley, A.P., and Engel, A. (2000). Domain structure of secretin PulD revealed by limited proteolysis and electron microscopy. EMBO J. *19*, 2229–2236.

Reichow, S.L., Korotkov, K.V., Hol, W.G., and Gonen, T. (2010). Structure of the cholera toxin secretion channel in its closed state. Nat. Struct. Mol. Biol. *17*, 1226–1232.

Religa, T.L., Markson, J.S., Mayor, U., Freund, S.M., and Fersht, A.R. (2005). Solution structure of a protein denatured state and folding intermediate. Nature *437*, 1053–1056.

Rodionova, N.A., Tatulian, S.A., Surrey, T., Jähnig, F., and Tamm, L.K. (1995). Characterization of two membrane-bound forms of OmpA. Biochemistry *34*, 1921–1929.

Spagnuolo, J., Opalka, N., Wen, W.X., Gagic, D., Chabaud, E., Bellini, P., Bennett, M.D., Norris, G.E., Darst, S.A., Russel, M., and Rakonjac, J. (2010). Identification of the gate regions in the primary structure of the secretin pIV. Mol. Microbiol. *76*, 133–150.

Spreter, T., Yip, C.K., Sanowar, S., André, I., Kimbrough, T.G., Vuckovic, M., Pfuetzner, R.A., Deng, W., Yu, A.C., Finlay, B.B., et al. (2009). A conserved structural motif mediates formation of the periplasmic rings in the type III secretion system. Nat. Struct. Mol. Biol. *16*, 468–476.

Tilley, S.J., and Saibil, H.R. (2006). The mechanism of pore formation by bacterial toxins. Curr. Opin. Struct. Biol. *16*, 230–236.

Vallée-Bélisle, A., and Michnick, S.W. (2012). Visualizing transient protein-folding intermediates by tryptophan-scanning mutagenesis. Nat. Struct. Mol. Biol. *19*, 731–736.

Van der Meeren, R., Wen, Y., Van Gelder, P., Tommassen, J., Devreese, B., and Savvides, S.N. (2013). New insights into the assembly of bacterial secretins: structural studies of the periplasmic domain of XcpQ from Pseudomonas aeruginosa. J. Biol. Chem. *288*, 1214–1225.